Changing Northern Hemisphere storm tracks in an ensemble of IPCC climate change simulations

Article

Published Version

Changing Northern Hemisphere Storm Tracks in an Ensemble of IPCC Climate Change Simulations

U. ULBRICH

Institute for Meteorology, Freie Universität Berlin, Berlin, Germany

J. G. PINTO

Institute for Geophysics and Meteorology, University of Cologne, Cologne, Germany

H. KUPFER, G. C. LECKEBUSCH, AND T. SPANGEHL

Institute for Meteorology, Freie Universität Berlin, Berlin, Germany

M. REYERS

Institute for Geophysics and Meteorology, University of Cologne, Cologne, Germany

(Manuscript received 13 April 2007, in final form 5 July 2007)

ABSTRACT

Winter storm-track activity over the Northern Hemisphere and its changes in a greenhouse gas scenario (the Special Report on Emission Scenarios A1B forcing) are computed from an ensemble of 23 single runs from 16 coupled global climate models (CGCMs). All models reproduce the general structures of the observed climatological storm-track pattern under present-day forcing conditions. Ensemble mean changes resulting from anthropogenic forcing include an increase of baroclinic wave activity over the eastern North Atlantic, amounting to 5%–8% by the end of the twenty-first century. Enhanced activity is also found over the Asian continent and over the North Pacific near the Aleutian Islands. At high latitudes and over parts of the subtropics, activity is reduced. Variations of the individual models around the ensemble average signal are not small, with a median of the pattern correlation near $r = 0.5$. There is, however, no evidence for a link between deviations in present-day climatology and deviations with respect to climate change.

1. Introduction

Cyclones and the associated baroclinic waves are key features of midlatitude weather and climate. Their occurrence, tracks, and intensities are most relevant for both climate means (e.g., Knappenberger and Michaels 1993; Hurrell 1995; Rogers 1997; Trigo et al. 2000), and for the generation of extreme events (e.g., Ulbrich et al. 2001, 2003a,b; Mudelsee et al. 2004). Their consideration in numerical models can provide insight into the mechanisms of simulated present-day variability and to anthropogenic climate change as simulated under the respective scenarios.

Corresponding author address: U. Ulbrich, Institute for Meteorology, Freie Universität Berlin, Carl-Heinrich-Becker-Weg 6-10, 12165 Berlin, Germany.
E-mail: ulbrich@met.fu-berlin.de

DOI: 10.1175/2007JCLI1992.1

While the former Intergovernmental Panel on Climate Change (IPCC) report (Houghton et al. 2001, p. 73) stated that there was little agreement among models concerning future changes in storm intensity, frequency, and variability, the IPCC AR4 (Solomon et al. 2007) mentions that "extra-tropical storm tracks are projected to move poleward, with consequent changes in wind, precipitation, and temperature patterns, continuing the broad pattern of observed trends over the last half-century." This summarizes a number of recent scientific results cited in the report. Below, we highlight some of the recent publications on this issue, including both studies for present-day and future climate, which are based on single model runs, on ensembles of runs with the same GCM, and on multimodel ensembles.

Yin (2005) presented a consistent poleward and upward shift and intensification of the zonal mean storm tracks in a 15-member multimodel ensemble, using the

TABLE 1. Models considered in the current study.

Name (IPCC identification)	Institute	Country	Resolution	Reference
CCCma (T47)	Canadian Centre for Climate Modeling and Analysis	Canada	T47 3.75° × 3.75° 31 level	Flato et al. (2000); Canadian Centre for Climate Modeling and Analysis (2005)
CCCma (T63)	Canadian Centre for Climate Modeling and Analysis	Canada	T63 ~2.8° × 2.8° 31 level	Flato et al. (2000); Canadian Centre for Climate Modeling and Analysis (2005)
CNRM-CM3	Météo-France/Centre National de Recherches Météorologiques	France	~2.8° × 2.8° 45 level	D. Salas-Mélia et al. (2005, personal communication)
CSIRO-Mk3.0	Commonwealth Scientific and Industrial Research Organisation (CSIRO) Atmospheric Research	Australia	T63 1.875° × 1.875° 18 level	Gordon et al. (2002)
ECHAM5/OM1	Max Planck Institute for Meteorology	Germany	T62 19 level	Jungclaus et al. (2006)
ECHO-G	Meteorological Institute of the University of Bonn, Meteorological Research Institute of KMA, and Model and Data Group	Germany/ Korea	T30 3.75° × 3.75° 19 level	Legutke and Voss (1999); Min et al. (2005)
FRA IPSL-CM4	Institut Pierre Simon Laplace	France	2.5° × 3.75° 19 level	Hourdin et al. (2006); Marti et al. (2005)
GFDL-CM2.0	U.S. Department of Commerce/ National Oceanic and Atmospheric Administration (NOAA)/ Geophysical Fluid Dynamics Laboratory	United States	2.5° × 2.0° 24 level	Delworth et al. (2006); Gnanadesikan et al. (2006)
GISS-AOM	NASA Goddard Institute for Space Studies	United States	4° × 3° 12 level	Russell et al. (1995); Lucarini and Russell (2002)
GISS E-R	NASA Goddard Institute for Space Studies	United States	5° × 4° 15 level	Schmidt et al. (2006)
IAP FGOALS-g1.0	State Key Laboratory of Numerical Modeling for Atmospheric Sciences and Geophysical Fluid Dynamics/Institute of Atmospheric Physics	China	T42 ~2.8° × 2.8° 26 level	Yu et al. (2002, 2004)
INM-CM3.0	Institute for Numerical Mathematics	Russia	5° × 4° 21 level	Diansky and Volodin (2002)
MIROC3.2(hires)	Center for Climate System Research (the University of Tokyo), National Institute for Environmental Studies, and Frontier Research Center for Global Change (JAMSTEC)	Japan	T106 1.125° × 1.125° 56 level	Hasumi and Emori (2004)
MIROC3.2(medres)	Center for Climate System Research (the University of Tokyo), National Institute for Environmental Studies, and Frontier Research Center for Global Change (JAMSTEC)	Japan	T42 ~2.81° × 2.81° 20 level	Hasumi and Emori (2004)
MRI-CGCM2.3.2	Meteorological Research Institute	Japan	T42 30 level	Yukimoto et al. (2006)
NCAR CCSM3	National Center for Atmospheric Research	United States	T83 ~1.4° × 1.4° 26 level	Meehl et al. (2006); Collins et al. (2006)

2–8-day bandpass-filtered eddy kinetic energy. He found the largest changes in the upper midlatitude troposphere and lower stratosphere, but zonal mean wind stress at the surface also showed a poleward shift. A northern movement and intensification of the North Pacific storm track (estimated from precipitation data in a 10-member multimodel ensemble) and Aleutian low was also found by Salathé (2006), while Lambert and Fyfe (2006) did not find any apparent changes in the geographical distribution of events, as identified in a 13-member multimodel ensemble. Geng and Sugi (2003) found an increase in the number of intense cyclones, along with decreasing overall numbers for Northern Hemisphere summer and winter in a high-resolution (T106) scenario run performed with the model of the Japanese Meteorological Agency. These opposing tendencies in the total number of cyclone events versus the number of intense events were also identified for Northern Hemisphere winter as a whole in the study of Lambert and Fyfe (2006). Some studies point at regional differences in these trends. Geng and Sugi (2003), for example, found an increase in both the total number of cyclones and in their mean intensities for an area around the Aleutian Islands and for the eastern North Atlantic. Both Bengtsson et al. (2006) and Pinto et al. (2007b) presented increased winter cyclone intensities in these two regions, but no evidence of increasing intensities over the whole hemisphere.

Because extremes in surface winds are related to the occurrence of intense cyclones, it is also of interest to look at climate change signals in this quantity. Leckebusch and Ulbrich (2004), Fischer-Bruns et al. (2005), Leckebusch et al. (2006, 2007), and Pinto et al. (2007a) found an increase in wind extremes and related damages over parts of northwestern Europe in several scenario simulations based on the ECHAM5, ECHAM4/Hamburg Ocean Primitive (HOPE), ECHAM4/Ocean Isopycnal Model (OPYC3), Third Hadley Centre Coupled Ocean–Atmosphere General Circulation Model (HadCM3), and Third Hadley Centre Atmospheric Model version P (HadAM3P) GCMs.

In summary, the papers considering the effect of the anthropogenic climate change on midlatitude synoptic

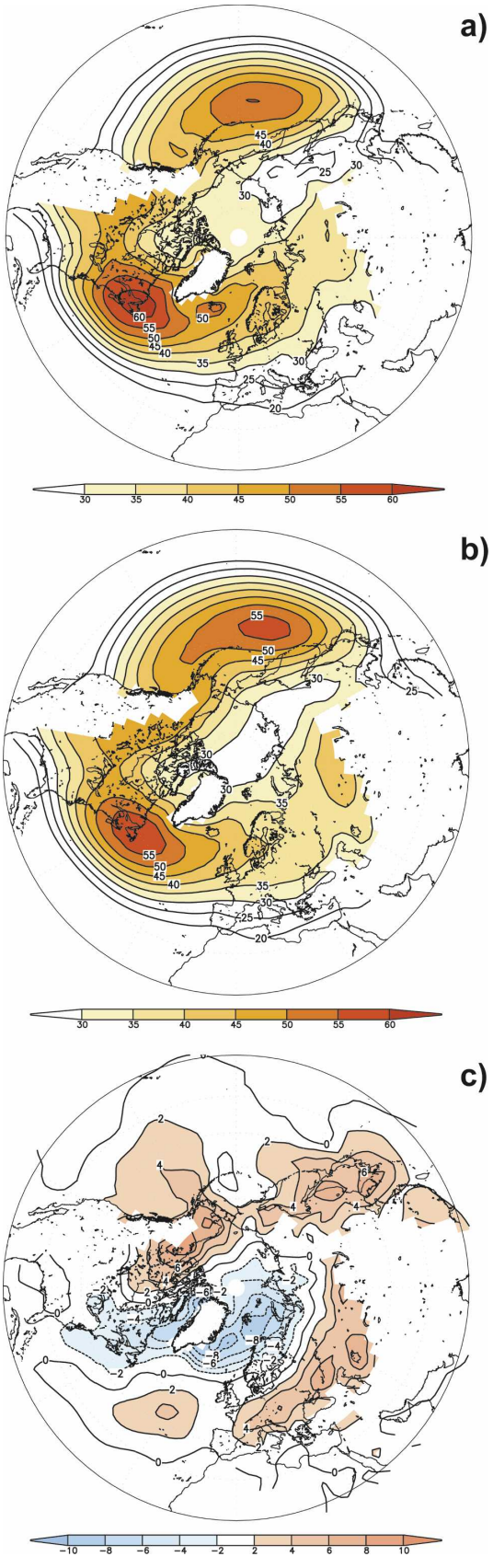

→

FIG. 1. (a) MSLP storm track in 1/10 hPa computed from NCEP–NCAR reanalysis 1961–2000; (b) same as (a), but from the GCM ensemble under present-day greenhouse forcing (20C, 1960–2000); and (c) difference ensemble mean minus NCEP–NCAR reanalysis. Values over high ground (>1000 m MSL) are omitted.

TABLE 2. Pattern correlations between storm-track activity patterns for present-day climate forcing (1960–2000). "Ensemble" signifies the 23 model run ensemble mean and NCEP is the pattern obtained from the NCEP–NCAR reanalysis of 1961–2000. Grid points at high ground (>1000 m MSL) are not used. Upper-right triangle of values: Northern Hemisphere; lower-left triangle of values: North Atlantic Window.

	CCCma	CCCma_T63	CNRM	CSIRO	ECHAM5	ECHO-G	FRA_IPSL	GFD	GISS_AOM
CCCma	1	0.99	0.97	0.98	0.98	0.99	0.97	0.98	0.95
CCCma_T63	0.98	1	0.98	0.97	0.98	0.99	0.97	0.98	0.95
CNRM	0.94	0.93	1	0.97	0.98	0.97	0.98	0.99	0.98
CSIROo	0.93	0.91	0.94	1	0.97	0.98	0.97	0.98	0.96
ECHAM5	0.95	0.96	0.96	0.91	1	0.98	0.98	0.99	0.97
ECHO-G	0.97	0.96	0.95	0.91	0.94	1	0.98	0.98	0.95
FRA_IPSL	0.92	0.93	0.95	0.89	0.96	0.93	1	0.99	0.97
GFD	0.97	0.94	0.98	0.93	0.97	0.95	0.95	1	0.98
GISS_AOM	0.9	0.86	0.95	0.89	0.93	0.88	0.91	0.96	1
GISS_E-R	0.86	0.89	0.84	0.78	0.89	0.86	0.88	0.86	0.84
IAP	0.79	0.87	0.8	0.74	0.84	0.85	0.87	0.77	0.7
INMCM	0.96	0.93	0.97	0.94	0.96	0.95	0.93	0.97	0.93
MIROC_h	0.99	0.97	0.95	0.93	0.97	0.95	0.92	0.97	0.93
MIROC_m	0.96	0.93	0.97	0.95	0.95	0.95	0.93	0.98	0.94
MRI	0.86	0.8	0.82	0.84	0.76	0.87	0.73	0.83	0.77
NCAR	0.93	0.96	0.91	0.87	0.96	0.94	0.94	0.91	0.83
ENSEMBLE1	0.98	0.98	0.98	0.94	0.98	0.98	0.96	0.98	0.93
NCEP	0.96	0.98	0.91	0.89	0.95	0.94	0.92	0.93	0.86

activity produce an emerging picture of corroborating results, in spite of the remaining variety in detail arising from the following:

- different individual signals resulting from the different model(s) and model run(s) considered, which depend on the specific model considered and on the decadal variability superimposed on the anthropogenic signals;
- specific characteristics of different cyclone identification and tracking schemes;
- different measures quantifying the strength of midlatitude baroclinic wave activity; and
- opposing signal effects for intense and weaker cyclones, which lead to a dependence of results on the chosen thresholds.

In the present study, we use a multimodel ensemble of coupled global circulation model (CGCM) simulations collected for the so-called IPCC diagnostic exercise, exploring the model ensemble's representation of the observational horizontal storm-track pattern, the ensemble mean climate signal, and the individual models' deviations. Our work is related to the recent studies of Yin (2005) and Lambert and Fyfe (2006) who had focused on the zonal and hemispheric mean signals in synoptic activity.

2. Data

In the data archive for the IPCC diagnostic exercise, daily mean data out of the transient simulations are available for three periods. We have chosen to consider the period associated with present-day greenhouse gas forcing (1961–2000) and the period for the final two decades of the Special Report on Emission Scenarios (SRES) A1B scenario (2081–2100). Other scenarios are not considered in our present study, but according to results of Lambert and Fyfe (2006) and Pinto et al. (2007b) the signals typically increase with increasing forcing. The models considered are listed in Table 1. Multiple runs were available for four of the models and thus are included in the ensemble. These models are CCCma (three runs), ECHAM5 (2 runs), Flexible Global Ocean–Atmosphere–Land System Model (IAP; three runs), and National Center for Atmospheric Research (NCAR; three runs). A validation of the models focused on mean sea level pressure (MSLP; particularly over central Europe) can be found in Van Ulden and van Oldenborgh (2006).

Because of the large amount of data featuring slightly different spatial resolutions and their availability only as daily averages, we refrained from a thorough identification of cyclones and their tracks. Instead, we use a simple approach for the quantification of synoptic wave activity ("storm track") after Blackmon (1976) and Blackmon et al. (1977). It was originally defined as the standard deviation of the bandpass- (2–6 days) filtered variability of 500-hPa geopotential heights, thus representing the sequence of upper-air troughs and ridges as the tropospheric counterparts of the surface cyclones and high pressure systems (Wallace and Gutzler 1981; Blackmon et al. 1984a,b; Wallace et al. 1988). Because

TABLE 2. *(Extended)*

GISS_E-R	IAP	INMCM	MIROC_h	MIROC_m	MRI	NCAR	ENSEMBLE1	NCEP
0.94	0.91	0.98	0.99	0.99	0.97	0.97	0.99	0.99
0.95	0.95	0.97	0.99	0.98	0.95	0.98	0.99	0.99
0.95	0.94	0.98	0.97	0.98	0.94	0.97	0.99	0.97
0.93	0.89	0.97	0.98	0.98	0.96	0.96	0.98	0.97
0.97	0.95	0.98	0.99	0.98	0.94	0.99	0.99	0.99
0.94	0.92	0.97	0.99	0.98	0.98	0.97	0.99	0.98
0.94	0.92	0.96	0.98	0.98	0.95	0.97	0.99	0.97
0.96	0.93	0.98	0.99	0.99	0.96	0.98	1	0.98
0.96	0.91	0.96	0.96	0.97	0.92	0.96	0.98	0.95
1	0.95	0.94	0.95	0.94	0.89	0.97	0.97	0.96
0.86	1	0.92	0.92	0.92	0.84	0.97	0.95	0.94
0.83	0.76	1	0.98	0.98	0.95	0.97	0.99	0.97
0.88	0.78	0.95	1	0.99	0.96	0.98	0.99	0.99
0.82	0.75	0.97	0.97	1	0.96	0.97	0.99	0.97
0.61	0.52	0.86	0.84	0.87	1	0.93	0.96	0.95
0.9	0.93	0.91	0.92	0.89	0.71	1	0.99	0.98
0.9	0.86	0.97	0.98	0.97	0.83	0.96	1	0.99
0.92	0.85	0.93	0.96	0.91	0.77	0.96	0.97	1

the IPCC data archive used does not contain daily height data for the 500-hPa level, we decided to perform the respective computations based on the available MSLP data. Note that the storm track is not affected by changes in the long-term mean MSLP (in contrast to cyclone core depth) so that changes can directly be assigned to the transient waves. Because it includes variability of both high and low surface pressure systems it should be distinguished from results of feature- (mostly cyclone) tracking schemes partly also operating with MSLP data. Grid points at high orography (>1000 m MSL) were excluded from all consideration to avoid a possible influence of extensive extrapolation below ground. The models' representation of present-day climate was validated using the National Centers for Environmental Prediction (NCEP)–NCAR reanalysis (Kalnay et al. 1996) for the period of 1958/59–1997/98.

3. Results

The mean MSLP storm-track pattern obtained from the model ensemble (Fig. 1b) is very similar to its observational counterpart (NCEP–NCAR reanalysis data for the period of 1960–99; see Fig. 1a). In particular, the storm-track maxima over the North Pacific (with maximum values of about 5 hPa southeast of the Kamchatka Peninsula) and over the North Atlantic (maximum values of about 6 hPa near Newfoundland) are well met by the ensemble mean. There is some underestimation of the model storm tracks in the Norwegian Sea area (Fig. 1c), associated with what is commonly referred to as "zonalization" of the GCMs, that is, the North Atlantic storm track is too zonally oriented (e.g., Doblas-Reyes et al. 1998). While Lucarini et al. (2007) suggest that the IPCC models typically overestimate the traveling baroclinic waves (considering meridional wind at the 500-hPa level) we find no clear evidence for such a general bias in the MSLP storm track. The agreement of the simulated storm-track pattern with its NCEP counterpart can be quantified by pattern correlations over all Northern Hemisphere grid points. All 16 models are able to reproduce the observed storm-track pattern, with correlation coefficients ranging from 0.94 to 0.99 for the individual models, and $r = 0.99$ for the ensemble mean (cf. Table 2, last column). Given the good agreement of the ensemble mean pattern with observational results, it is not unexpected that the models with low agreement with respect to NCEP (these are IAP, MRI, GISS_AOM) are also on the lower side with respect to the ensemble mean (Table 2, second last column). For a more detailed diagnosis, maps of the individual models' deviations from the ensemble mean can be considered.[1] It is found that the absolute differences to the ensemble mean are rather large for these three models, but the areas and signatures of the deviations do not agree. In fact,

[1] Supplemental information related to this paper is available at the Journals Online Web site: http://dx.doi.org/10.1175/2007JCLI1992.s1.

the MRI and IAP have deviations with opposing signs, which is also reflected in the low value of the pattern correlation for this model pair ($r = 0.84$; see Table 2, values in the upper-right triangle). It should be noted, however, that the agreement between the pairs of individual present-day storm-track patterns is generally lower than the agreement with the ensemble mean.

Limiting the evaluation of the individual models' representation of the storm tracks to grid points in the North Atlantic window (30°–70°N, 90°W–60°E), we find pattern correlations in a range between $r = 0.77$ and 0.98 (cf. Table 2, last row). In this case, the ensemble mean is marginally worse in meeting the observational data than the best single model (CCCma_t63), but the difference is small. The model combination with the worst agreement of the simulated patterns is again MRI and IAP ($r = 0.52$).

Climate change signals are defined as the difference between climatological storm-track means for the SRES A1B scenario period of 2081–2100 and the control period of 1960–2000. A local statistical significance at individual grid points is estimated from a simple t test, using the variability of storm-track intensities in individual model winters. The ensemble mean signal (Fig. 2) reveals regions with enhanced storm-track activity over the northern North Pacific and eastern North Atlantic. Over the eastern North Atlantic (between the Azores and the British Isles) an increase of 5%–8% over the models' present-day values is found. This region is located downstream and partly south of the respective climatological storm-track maximum. Over the North Pacific (near the Aleutian Islands), the region with increasing values and about the same relative changes is located close to the climatological storm-track maximum. Over the Asian continent, there are also areas with enhanced activity. While they were partly omitted from the figures and computations because they are located at high orography, it should be noted that increasing storm-track activity at upper levels was detected over Asia in scenario runs with one of the models (ECHAM5; see Pinto et al. 2007b), indicating that local positive signals over the Asian continent should not be rated an artifact of extrapolation. There are also areas of the Northern Hemisphere where storm-track activity decreases under increasing greenhouse gas forcing, namely, the high latitudes, areas over North Africa, the southwestern North Pacific, and the Gulf of Mexico. The degree of agreement between the signal patterns of the individual models and the ensemble mean is quantified by computing the respective pattern correlations (Table 3). All signals but one are positively correlated to the ensemble mean signal (for IAP $r = -0.23$), but for some of the models the correlation is rather modest, so that the median value is only about 0.5. The model agreeing best with the ensemble mean signal pattern is ECHAM5 ($r = 0.71$). Correlations between signals from individual models are generally not high, and there is a considerable number (over 25%) of anticorrelated signal pattern pairs [e.g., IAP and CNRM, $r = -0.54$]. For the North Atlantic window, qualitatively similar results to those for the Northern Hemisphere are obtained. Pattern correlations between the climate signals of the IAP and the ensemble mean are again as low as $r = -0.49$. This originates from a climate signal in the IAP model over the eastern North Atlantic, which is largely opposite to the ensemble mean signal there.[2] This deviation is, however, not apparently related to the deviation with respect to present-day climatology (as shown in the first supplement, online at http://dx.doi.org/10.1175/2007JCLI1992.s1). This is a more general result that is also valid for other models, suggesting that the deviation in present-day climatology is not related to the deviation in the climate signal.

As mentioned earlier, for some models more than one run entered the computations. For the intercomparison of patterns discussed earlier, only the mean of the contributing runs had been used. Comparing now the climate change patterns of these model runs with those of the multimodel ensemble, the agreement between the different runs of the same model on a hemispheric scale is only marginally better than that between the different GCMs. Between the CCCMA runs, the correlations of the climate change patterns range between 0.08 and 0.56, for IAP between 0.69 and 0.8, and for NCEP–NCAR between 0.31 and 0.41. For the ECHAM5 model, the pattern correlation between the two runs is 0.31. The large variability between the signals from individual runs is most likely an effect of the rather short averaging periods (consisting of only 20 winters for the scenario period), which are strongly influenced by the interannual and interdecadal variability in the model runs (Räisänen 2001; see also Fig. 6 in Pinto et al. 2007b for an example). More generally, variations between different ensemble members of the same model are smaller than variations between different models (Sorteberg and Kvamstø 2006).

[2] Supplemental information related to this paper is available at the Journals Online Web site: http://dx.doi.org/10.1175/2007JCLI1992.s2.

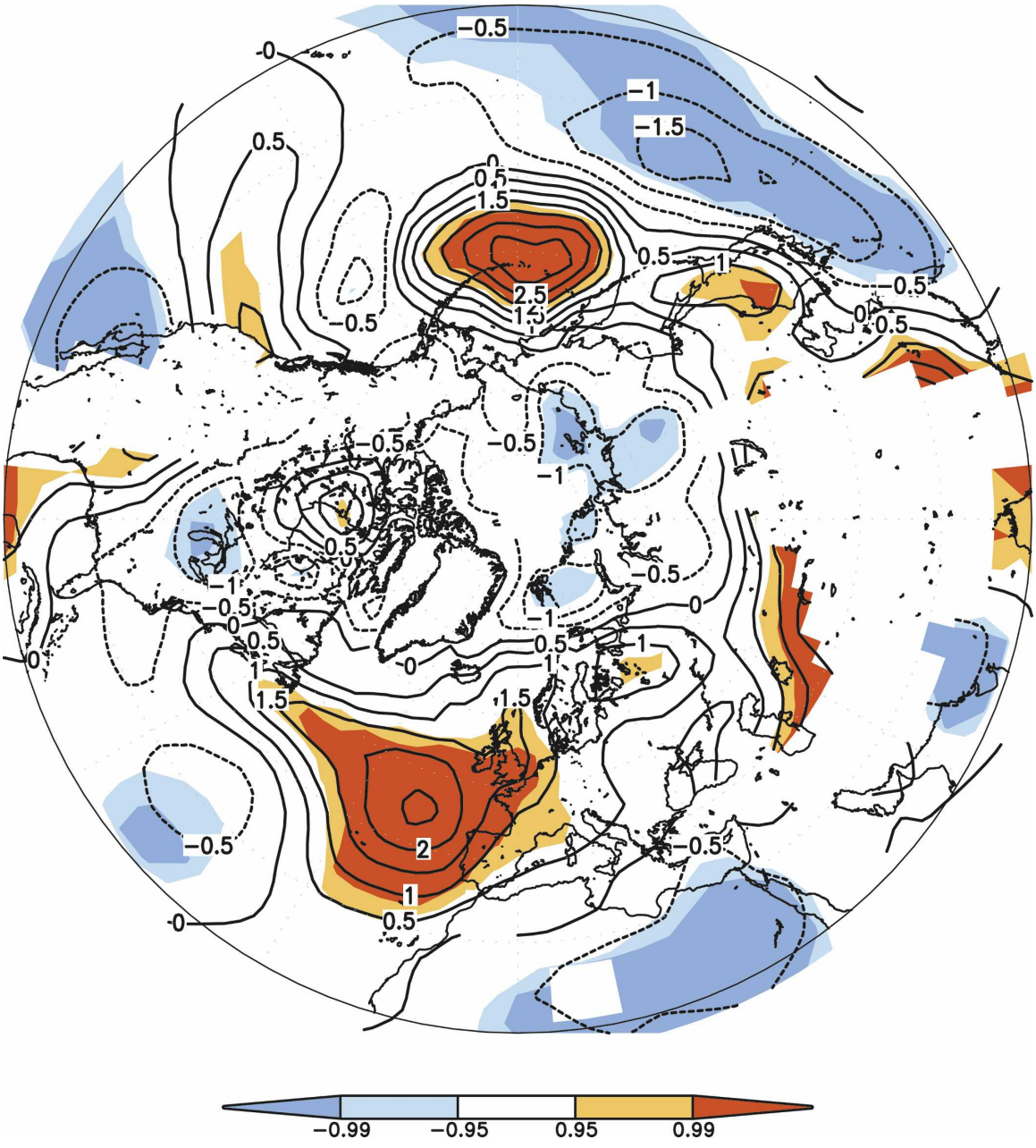

FIG. 2. Greenhouse gas signal for MSLP storm track in 1/10 hPa, computed as the difference between the forcing period of SRES A1B (2080–2100) and the present-day forcing (1960–2000). Values over high ground (>1000 m MSL) are omitted. Significant differences at 95% (and 99%) confidence levels are in color, with a *t* test on the winter basis.

4. Concluding remarks

We have investigated a 23-member ensemble of simulations performed with 16 different GCMs for the present day and for future (scenario A1b) climate forcing in terms of storm-track activity, computed from daily mean MSLP data. With respect to present-day climate, the models perform well in reproducing the observed climatological pattern. The ensemble mean performs as good as the single individual model closest to the NCEP–NCAR climatology. The climate change signal for the model ensemble provides evidence for increasing storm-track activity in the eastern North Atlantic/western Europe, the North Pacific, and parts of the Asian continent. Many individual model signals are only in modest agreement with the common signal,

TABLE 3. Pattern correlations between storm-track activity changes (differences between averages for the 2080–2100 Alb forcing period and the 1960–2000 present-day forcing period). Grid points at high ground (>1000 m MSL) are not used. Upper-right triangle: Northern Hemisphere; lower-left triangle: North Atlantic window.

	CCCma	CCCma_T63	CNRM	CSIRO	ECHAM5	ECHO-G	FRA_IPSL	GFD	GISS_AOM
CCCma	1	0.35	0.21	0.24	0.35	0.1	−0.19	0.34	0.41
CCCma_T63	0.19	1	−0.16	0.23	0.19	−0.48	−0.13	0.01	0.2
CNRM	0.11	−0.07	1	0.15	0.34	0.5	0.22	0.24	0.45
CSIROo	0.24	0.14	0	1	0.35	0.05	0.07	0.18	0.24
ECHAM5	0.19	0.06	0.58	0.2	1	0.02	0.06	0.33	0.48
ECHO-G	0.21	−0.42	0.23	0.24	0.13	1	0.36	0.2	0.33
FRA_IPSL	−0.32	0.03	0.02	−0.09	−0.09	0.46	1	−0.18	0.03
GFD	0.5	−0.2	0.38	0.23	0.5	0.25	−0.41	1	0.34
GISS_AOM	0.27	0.16	0.47	0.37	0.45	0.39	0.11	0.46	1
GISS_E-R	0.18	0.24	0.34	−0.01	0.43	−0.5	−0.53	0.21	0.04
IAP	−0.4	−0.1	−0.5	−0.14	−0.28	−0.43	−0.27	−0.25	−0.49
INMCM	0.58	0.04	−0.08	0.38	0.18	0.18	−0.37	0.33	0.29
MIROC_h	0.63	0.29	0.16	0.19	0.17	0.08	−0.13	0.14	0.3
MIROC_m	0.42	−0.22	0.21	0.49	0.45	0.35	−0.39	0.77	0.45
MRI	−0.13	0.63	0.13	−0.06	−0.08	−0.49	0	−0.24	0.19
NCAR	0.15	0.51	0.39	0.16	0.66	−0.15	0	0.14	0.47
ENSEMBLE1	0.53	0.28	0.58	0.49	0.7	0.36	−0.01	0.57	0.81

but only one of the models has a negative correlation with the ensemble mean signal pattern. This is the same model, which is worst in representing the observed storm-track pattern, but we also found other models with rather low agreement, and so there was no obvious justification to treat it as an outlier. We have also compared signal patterns from pairs of individual models, finding that negative pattern correlations occur for several such pairs. It is also noted that the individual models' deviations from the ensemble mean signal (see the second online supplement at http://dx.doi.org/10.1175/2007JCLI1992.s2) do not apparently reflect deviations in present-day climatology (see the first online supplement at http://dx.doi.org/10.1175/2007JCLI1992.s1).

Comparison with other studies suggests that the regional increase we found for the storm track at sea level is exceeded in intensity and zonal extension by the signals at upper levels: Yin (2005) considered the zonal mean storm-track signal in a multimodel ensemble obtained from the same data source as used in the present study, and found evidence that the increase of the signal with height is caused by increasing baroclinicity. Note, however, that even though our results show poleward shifts of storm-track activity in some areas (e.g., the North Pacific), they do not resemble the clear poleward shift of zonal mean eddy activity in the upper troposphere found by Yin (2005). Pinto et al. (2007b) considered the storm-track signal at 500 hPa in a small ensemble performed with the ECHAM5 model, that is, the model identified in the present study as the one with the best agreement of the climate change signal with the ensemble mean. They showed a 500-hPa storm-track signal that is extending downstream from the areas of maximum increase in the Atlantic into the Asian continent, thus linking the areas of increasing activity at the surface. Note that the ECHAM5 model also features a very good representation of the MSLP fields (Van Ulden and van Oldenborgh 2006).

Our results seem to corroborate estimates based on climate projections, which indicate an increasing storm risk over western Europe under climate change (Pinto et al. 2006, 2007a,b; Leckebusch et al. 2006, 2007). The ECHAM5 model is one of the GCMs providing the basis for these suggestions. It appears that a physical interrelation between increasing storm-track activity, intensifying extreme cyclones, and windstorm events could be evident. One should bear in mind, however, that the area of intensifying storm-track activity (related to the sequence of local high and low pressures) cannot be interpreted as an area of increased windstorm risk. For the ECHAM5 A1B scenario, for example, the area with significantly increasing extreme wind storms (Pinto et al. 2007b, their Fig. 9b) is largely located downstream of the area with increasing storm-track activity in the eastern North Atlantic (not shown, cf. Fig. 2 and the ECHAM5 deviations shown in http://dx.doi.org/10.1175/2007JCLI1992.s2).

Using ensembles should minimize the insecurity arising from natural climate variability as it is produced by the models. This variability requires that either longer time series and/or larger ensembles of model runs are produced and evaluated. Finding similar correlations between the climate change patterns from runs pro-

TABLE 3. *(Extended)*

GISS_E-R	IAP	INMCM	MIROC_h	MIROC_m	MRI	NCAR	ENSEMBLE1
0.25	−0.23	0.38	0.46	0.25	0.06	0.27	0.55
0.17	0.24	0.39	0.3	−0.26	0.24	0.5	0.31
0.27	−0.54	−0.06	0.18	0.33	0.16	0.05	0.54
0.32	−0.16	0.13	0.4	0.26	0.12	0.13	0.52
0.56	−0.21	0.12	0.54	0.27	0.25	0.54	0.71
−0.16	−0.49	−0.13	−0.04	0.5	−0.17	−0.27	0.32
0.23	−0.39	−0.31	0.06	−0.17	0.23	−0.15	0.11
0.18	−0.02	0.19	0.07	0.46	−0.1	0.1	0.47
0.2	−0.3	0.23	0.36	0.3	0.16	0.33	0.7
1	−0.09	0.24	0.49	0.22	0.33	0.41	0.57
0.04	1	0.41	−0.25	−0.31	−0.25	0.15	−0.23
0.2	−0.21	1	0.2	−0.03	−0.23	0.34	0.39
0.19	−0.33	0.32	1	0.06	0.23	0.33	0.6
0.11	−0.23	0.58	0.07	1	−0.01	0.03	0.46
0.23	0.02	−0.28	0.11	−0.4	1	0.31	0.32
0.49	−0.31	0.23	0.25	0.14	0.36	1	0.51
0.32	−0.49	0.45	0.49	0.56	0.13	0.66	1

duced with the same GCM on the one hand, and the respective intermodel correlations on the other hand, we suggest that the 20-yr scenario period that is used is still a bit short for adequately dealing with temporal variability. With respect to our approach of including all available models with equal weight, one could argue that excluding outliers from the ensemble could produce more consistent results. Their identification (either from their representation of present-day climatology or from the agreement of climate signals with the ensemble mean, e.g.), however, is not unambiguous. A thorough investigation into the reasons for a model's seemingly bad representation of present-day climate, or for a signal that contradicts many other models, is the more adequate way to deal with this part of insecurity about climate change [see, e.g., Greeves et al. (2007) for an assessment of storm-track sensitivities arising from the formulation of the Hadley Centre's models dynamical cores and resolution].

The current paper demonstrated that a common greenhouse gas signal can be identified from an ensemble of model simulation, using a specific quantification measure for storm-track activity. After asking what causes the impression of diverging results in different studies on changing storm tracks, we think that the different approaches used for quantifying them are part of the story. In general, the existence of the different approaches to study storm tracks is well justified, because "mid-latitude storms are complicated features and as such require a variety of analytical methods to assess their representation in models" (Greeves et al. 2007). Because the different analytical methods highlight different aspects of the storm tracks, they do not necessarily have to produce identical climatological or climate change patterns [in spite of usage of the same data source; see, e.g, Hoskins and Hodges (2002)]. Further work is needed to understand these differences, because they can help to understand this part of the physical climate system and its sensitivity to rising greenhouse gas concentrations [see Jiang and Perrie (2007) for a recent example of such an investigation].

Acknowledgments. We acknowledge the modeling groups for providing their data for analysis, the Program for Climate Model Diagnosis and Intercomparison (PCMDI) for collecting and archiving the model output, and the JSC/CLIVAR Working Group on Coupled Modelling (WGCM) for organizing the model data analysis activity. The multimodel data archive is supported by the Office of Science, U.S. Department of Energy. The work was partly supported by the European Union in the ENSEMBLES project (Contract GOCE-CT-2003-505593-ENSEMBLES) and by the German research ministry Grant "Collaborative Climate Computing Grid (C3-Grid)" under Grant 01AK801E. Computations were carried out at the Centre for applied informatics (ZAIK) of the University of Cologne. We thank two anonymous reviewers for their comments, which helped to improve the paper.

REFERENCES

Bengtsson, L., K. I. Hodges, and E. Roeckner, 2006: Storm tracks and climate change. *J. Climate,* **19,** 3518–3543.

Blackmon, M. L., 1976: A climatological spectral study of the

500 mb geopotential height of the Northern Hemisphere. *J. Atmos. Sci.,* **33,** 1607–1623.

——, J. M. Wallace, N.-C. Lau, and S. L. Mullen, 1977: An observational study of the Northern Hemisphere wintertime circulation. *J. Atmos. Sci.,* **34,** 1040–1053.

——, Y.-H. Lee, and J. M. Wallace, 1984a: Horizontal structure of 500 mb height fluctuations with long, intermediate, and short time scales. *J. Atmos. Sci.,* **41,** 961–979.

——, ——, ——, and H.-H. Hsu, 1984b: Time variation of 500 mb height fluctuations with long, intermediate, and short time scales as deduced from lag-correlation statistics. *J. Atmos. Sci.,* **41,** 981–991.

Canadian Centre for Climate Modelling and Analysis, cited 2005: The third generation Coupled Global Climate Model (CGCM3). [Available online at http://www.cccma.ec.gc.ca/models/cgcm3.shtml.]

Collins, W. D., and Coauthors, 2006: The Community Climate System Model version 3 (CCSM3). *J. Climate,* **19,** 2122–2143.

Delworth, T. L., and Coauthors, 2006: GFDL's CM2 global coupled climate models. Part I: Formulation and simulation characteristics. *J. Climate,* **19,** 643–674.

Diansky, N. A., and E. M. Volodin, 2002: Simulation of present-day climate with a coupled atmosphere–ocean general circulation model. *Izv. Atmos. Ocean Phys.,* **38,** 732–747.

Doblas-Reyes, F. J., M. Déqué, F. Valero, and D. B. Stephenson, 1998: North Atlantic wintertime intraseasonal variability and its sensitivity to GCM horizontal resolution. *Tellus,* **50A,** 573–595.

Fischer-Bruns, I., H. von Storch, J. F. González-Rouco, and E. Zorita, 2005: Modeling the variability of midlatitude storm activity on decadal to century time scales. *Climate Dyn.,* **25,** 461–476.

Flato, G. M., G. J. Boer, W. G. Lee, N. A. McFarlane, D. Ramsden, M. C. Reader, and A. J. Weaver, 2000: The Canadian Centre for Climate Modelling and Analysis global coupled model and its climate. *Climate Dyn.,* **16,** 451–467.

Geng, Q. Z., and M. Sugi, 2003: Possible change of extratropical cyclone activity due to enhanced greenhouse gases and sulfate aerosols—Study with a high-resolution AGCM. *J. Climate,* **16,** 2262–2274.

Gnanadesikan, A., and Coauthors, 2006: GFDL's CM2 global coupled climate models. Part II: The baseline ocean simulation. *J. Climate,* **19,** 675–697.

Gordon, H. B., and Coauthors, 2002: The CSIRO Mk3 Climate System Model. CSIRO Atmospheric Research Tech. Rep. 60, 130 pp.

Greeves, C. Z., V. D. Pope, R. A. Stratton, and G. M. Martin, 2007: Representation of Northern Hemisphere winter storm tracks in climate models. *Climate Dyn.,* **28,** 683–702.

Hasumi, H., and S. Emori, 2004: K-1 coupled model (MIROC) description. Center for Climate System Research, University of Tokyo, K-1 Tech. Rep. 1, 34 pp.

Hoskins, B. J., and K. I. Hodges, 2002: New perspectives on the Northern Hemisphere winter storm tracks. *J. Atmos. Sci.,* **59,** 1041–1061.

Houghton, J. T., Y. Ding, D. J. Griggs, M. Noguer, P. J. van der Linden, X. Dai, K. Maskell, and C. A. Johnson, Eds., 2001: *Climate Change 2001: The Scientific Basis*. Cambridge University Press, 881 pp.

Hourdin, F., and Coauthors, 2006: The LMDZ4 general circulation model: Climate performance and sensitivity to parametrized physics with emphasis on tropical convection. *Climate Dyn.,* **27,** 787–813.

Hurrell, J. W., 1995: Transient eddy forcing of the rotational flow during northern winter. *J. Atmos. Sci.,* **52,** 2286–2301.

Jiang, J., and W. Perrie, 2007: The impacts of climate change on autumn North Atlantic midlatitude cyclones. *J. Climate,* **20,** 1174–1187.

Jungclaus, J. H., and Coauthors, 2006: Ocean circulation and tropical variability in the coupled model ECHAM5/MPI-OM. *J. Climate,* **19,** 3952–3972.

Kalnay, E., and Coauthors, 1996: The NCEP/NCAR 40-Year Reanalysis Project. *Bull. Amer. Meteor. Soc.,* **77,** 437–471.

Knappenberger, P. C., and P. J. Michaels, 1993: Cyclone tracks and wintertime climate in the mid-Atlantic region of the USA. *Int. J. Climatol.,* **13,** 509–531.

Lambert, S. J., and J. C. Fyfe, 2006: Changes in winter cyclone frequencies and strengths simulated in enhanced greenhouse warming experiments: Results from the models participating in the IPCC diagnostic exercise. *Climate Dyn.,* **26,** 713–728.

Leckebusch, G. C., and U. Ulbrich, 2004: On the relationship between cyclones and extreme windstorms over Europe under climate change. *Global Planet. Change,* **44,** 181–193.

——, B. Koffi, U. Ulbrich, J. G. Pinto, T. Spangehl, and S. Zacharias, 2006: Analysis of frequency and intensity of European winter storm events from a multi-model perspective, at synoptic and regional scales. *Climate Res.,* **31,** 59–74.

——, U. Ulbrich, E. L. Fröhlich, and J. G. Pinto, 2007: Property loss potentials for European mid-latitude storms in a changing climate. *Geophys. Res. Lett.,* **34,** L05703, doi:10.1029/2006GL027663.

Legutke, S., and R. Voss, 1999: The Hamburg atmosphere–ocean coupled circulation model ECHO-G. German Climate Computing Center (DKRZ) Tech. Rep. 18, 62 pp.

Lucarini, V., and G. L. Russell, 2002: Comparison of mean climate trends in the Northern Hemisphere between National Centers for Environmental Prediction and two atmosphere–ocean model forced runs. *J. Geophys. Res.,* **107,** 4269, doi:10.1029/2001JD001247.

——, S. Calmanti, A. Dell'Aquila, P. M. Ruti, and A. Speranza, 2007: Intercomparison of the Northern Hemisphere winter mid-latitude atmospheric variability of the IPCC models. *Climate Dyn.,* **28,** 829–848.

Marti, O., and Coauthors, 2005: The new IPSL climate system model: IPSL-CM4. Note du Pole de Modelisation 26, Institut Pierre Simon Laplace, 84 pp. [Available online at http://dods.ipsl.jussieu.fr/omamce/IPSLCM4/DocIPSLCM4/FILES/DocIPSLCM4.pdf.]

Meehl, G. A., and Coauthors, 2006: Climate change projections for the twenty-first century and climate change commitment in the CCSM3. *J. Climate,* **19,** 2597–2616.

Min, S.-K., S. Legutke, A. Hense, and W.-T. Kwon, 2005: Internal variability in a 1000-year control simulation with the coupled climate model ECHO-G. Part I: Near surface temperature, precipitation, and mean sea level pressure. *Tellus,* **57A,** 605–621.

Mudelsee, M., M. Börngen, G. Tetzlaff, and U. Grünewald, 2004: Extreme floods in central Europe over the past 500 years: Role of cyclone pathway "Zugstrasse Vb." *J. Geophys. Res.,* **109,** D23101, doi:10.1029/2004JD005034.

Pinto, J. G., T. Spangehl, U. Ulbrich, and P. Speth, 2006: Assessment of winter cyclone activity in a transient ECHAM4-OPYC3 GHG experiment. *Meteor. Z.,* **15,** 279–291.

——, E. L. Fröhlich, G. C. Leckebusch, and U. Ulbrich, 2007a: Changing European Storm loss potentials under modified climate conditions according to ensemble simulations of the

ECHAM5/MPI-OM1 GCM. *Nat. Hazards Earth Syst. Sci.,* **7,** 165–175.

——, U. Ulbrich, G. C. Leckebusch, T. Spangehl, M. Reyers, and S. Zacharias, 2007b: Changes in storm track and cyclone activity in three SRES ensemble experiments with the ECHAM5/MPI-OM1 GCM. *Climate Dyn.,* **29,** 195–210.

Räisänen, J., 2001: CO_2-induced climate change in CMIP2 experiments: Quantification of agreement and role of internal variability. *J. Climate,* **14,** 2088–2104.

Rogers, J. C., 1997: North Atlantic storm track variability and its association to the North Atlantic Oscillation and climate variability of northern Europe. *J. Climate,* **10,** 1635–1647.

Russell, G. L., J. R. Miller, and D. Rind, 1995: A coupled atmosphere–ocean model for transient climate change studies. *Atmos.–Ocean,* **33,** 683–730.

Salas-Mélia, D., and Coauthors, 2005: Description and validation of the CNRM-CM3 global coupled model. CNRM, Note de Centre n 103, 36 pp. [Available online at http://www.cnrm.meteo.fr/scenario2004/paper_cm3.pdf.]

Salathé, E. P., Jr., 2006: Influences of a shift in North Pacific storm tracks on western North American precipitation under global warming. *Geophys. Res. Lett.,* **33,** L19820, doi:10.1029/2006GL026882.

Schmidt, G. A., and Coauthors, 2006: Present-day atmospheric simulations using GISS ModelE: Comparison to in situ, satellite, and reanalysis data. *J. Climate,* **19,** 153–192.

Solomon, S., D. Qin, M. Manning, Z. Chen, M. Marquis, K. B. Averyt, M. Tignor, and H. L. Miller, Eds., 2007: *Climate Change 2007: The Physical Science Basis.* Cambridge University Press, 996 pp.

Sorteberg, A. and N. G. Kvamstø, 2006: The effect of internal variability on anthropogenic climate projections. *Tellus,* **58A,** 565–574.

Trigo, I. F., T. D. Davies, and G. R. Bigg, 2000: Decline in Mediterranean rainfall caused by weakening of Mediterranean cyclones. *Geophys. Res. Lett.,* **27,** 2913–2916.

Ulbrich, U., A. Fink, M. Klawa, and J. G. Pinto, 2001: Three extreme storms over Europe in December 1999. *Weather,* **56,** 70–80.

——, T. Brücher, A. Fink, G. C. Leckebusch, A. Krüger, and J. G. Pinto, 2003a: The Central European floods in August 2002. Part 1: Rainfall periods and flood development. *Weather,* **58,** 371–377.

——, ——, ——, ——, ——, and ——, 2003b: The Central European floods in August 2002. Part 2: Synoptic causes and considerations with respect to climate change. *Weather,* **58,** 434–442.

Van Ulden, A. P., and G. J. van Oldenborgh, 2006: Large-scale atmospheric circulation biases and changes in global climate model simulations and their importance for climate change in Central Europe. *Atmos. Chem. Phys.,* **6,** 863–881.

Wallace, J. M., and D. S. Gutzler, 1981: Teleconnections in the geopotential height field during the Northern Hemisphere winter. *Mon. Wea. Rev.,* **109,** 784–812.

——, G.-H. Lim, and M. L. Blackmon, 1988: Relationship between cyclone tracks, anticyclone tracks, and baroclinic waveguides. *J. Atmos. Sci.,* **45,** 439–462.

Yin, J. H., 2005: A consistent poleward shift of the storm tracks in simulations of 21st century climate. *Geophys. Res. Lett.,* **32,** L18701, doi:10.1029/2005GL023684.

Yu, Y., R. Yu, X. Zhang, and H. Liu, 2002: A flexible coupled ocean–atmosphere general circulation model. *Adv. Atmos. Sci.,* **19,** 169–190.

——, X. Zhang, and Y. Guo, 2004: Global coupled ocean–atmosphere general circulation models in LASG/IAP. *Adv. Atmos. Sci.,* **21,** 444–455.

Yukimoto, S., and Coauthors, 2006: Present-day climate and climate sensitivity in the Meteorological Research Institute coupled GCM version 2.3 (MRI-CGCM2.3). *J. Meteor. Soc. Japan,* **84,** 333–363.